The Holocene

http://hol.sagepub.com

A mid-Holocene shift in Arctic sea-ice variability on the East Greenland Shelf

Anne E. Jennings, Karen Luise Knudsen, Morten Hald, Carsten Vigen Hansen and John T. Andrews

The Holocene 2002; 12; 49

DOI: 10.1191/0959683602hl519rp

A mid-Holocene shift in Arctic sea-ice variability on the East Greenland Shelf

Anne E. Jennings,[1]* Karen Luise Knudsen,[2] Morten Hald,[3] Carsten Vigen Hansen[2] and John T. Andrews[1]

([1]INSTAAR and Department of Geological Sciences, University of Colorado, Boulder, Colorado 80309–0450, USA; [2]Department of Earth Sciences, University of Aarhus, DK-8000, Århus, C, Denmark; [3]Department of Geology, University of Tromsø, N-9037 Tromsø, Norway)

Received 7 September 2000; revised manuscript accepted 23 April 2001

A
HOLOCENE
RESEARCH
PAPER

Abstract: Records of iceberg-rafting and palaeohydrography from two East Greenland shelf cores (JM96-1206/1-GC and JM96-1207/1-GC) are reported. Benthic foraminifera, stable isotopes and IRD fluxes indicate a shift toward colder, lower-salinity 'polar' conditions *c.* 5 cal. ka. A new proxy of iceberg-rafting on the East Greenland Shelf is the flux of calcium carbonate (TIC) thought to be derived from glacial erosion of Cretaceous calcareous mudstones. A change in the regularity and spacing of carbonate flux peaks at *c.* 4.7 cal. ka in JM96-1207 coincides with the onset of Neoglacial cooling in the Renland ice core $\delta^{18}O$ record. We propose that the carbonate flux peaks between 4.7 and 0.4 cal. ka are related to sea-surface coolings associated with increased flux of polar water and sea ice in the East Greenland Current. These peaks are synchronous with sea-surface coolings interpreted from North Atlantic deep-sea cores, but additional peaks centred around 2.4 and 3.8 cal. ka in JM96-1207 suggest that the shelf site captures higher-frequency events. The data indicate that severe Arctic sea-ice events began in the Neoglacial interval, and that earlier-Holocene cool events in deep-sea records are associated with other processes, such as release of meltwater from residual glacier ice and glacial lakes.

Key words: Neoglacial, sea ice, iceberg-rafting, benthic foraminifera, stable isotopes, mid-Holocene, Greenland.

Introduction

Variations in sea ice modulate global climate by influencing surface albedo, marine productivity, ocean-to-atmosphere heat and moisture fluxes, meridional heat transport into the northern North Atlantic, and the global thermohaline circulation (Aagaard and Carmack, 1994). Natural variability in the distribution and fluxes of sea ice and fresh water out of the Arctic Ocean can be inferred from geological and biological proxies measured in marine sediment cores. These data provide palaeoclimatic and palaeoenvironmental information beyond the instrumental record into time periods that precede strong anthropogenic influences (e.g., Aagaard *et al.*, 1991; McPhee *et al.*, 1998). The East Greenland Shelf is particularly sensitive to changes in sea ice and freshwater outflow from the Arctic Ocean because it underlies the East Greenland Current, which is one of the major sea-ice and freshwater export pathways from the Arctic Ocean (e.g., Jennings and Weiner, 1996). Proxy records of Holocene climate history on East Greenland are internally consistent at multicentury to millennial resolution (e.g., Andrews *et al.*, 1997). Holocene records show that, once deglaciation was complete, the climatic proxies follow the broad trends indicated by the solar insolation, such that early- to mid-Holocene warming was followed by Neoglacial cooling beginning between 6 and 4 cal. ka (e.g., Andrews *et al.*, 1997; Koç *et al.*, 1993; Keigwin, 1996). Records of ice-rafted detritus (IRD) from several shelf cores showed that between 8 and 6 cal. ka there were rare intervals of IRD delivery, whereas in the last 6 cal. ka the IRD was pervasive (Andrews *et al.*, 1997).

In this paper, we present multicentury- to century-scale reconstructions of postglacial Holocene palaeoceanography using sediment cores from the Nansen Trough, East Greenland Shelf (Figure 1). The sensitivity of the East Greenland Shelf to sea-ice variations is demonstrated in a study of Nansen Fjord cores that span the last 1300 years (Jennings and Weiner, 1996). These cores show large changes in polar water flux from the Arctic Ocean that parallel the history of the Arctic Sea ice incidence around Iceland (Ogilvie, 1984; Ogilvie *et al.*, 2000). Our focus in this paper is the mid-Holocene climatic shift from the low-IRD early Holocene to the high-IRD Neoglacial interval and its potential relation to sea-ice expansions into the North Atlantic and possible links to atmospheric circulation patterns. Measurements of changes in the composition and flux of ice-rafted detritus (IRD), the stable

*Author for correspondence (e-mail: jenninga@spot.colorado.edu)

10.1191/0959683602hl519rp

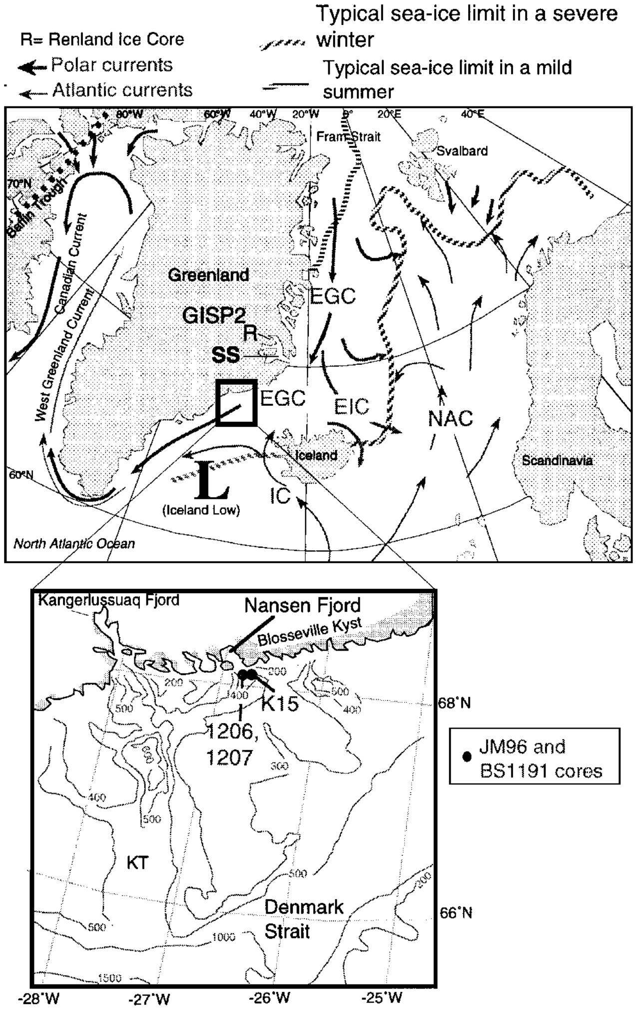

Figure 1 Top: map of Nordic Seas after Hurdle (1986). Bottom: location map showing Nansen Trough and core locations. Abbreviations are as follows: EGC = East Greenland Current; EIC = East Iceland Current; NAC = North Atlantic Current; IC = Irminger Current; KT = Kangerlussuaq Trough; R = Renland Ice Core; SS = Scoresby Sund; GISP2 = Greenland Ice Sheet Project 2 Ice Core. Contours are in metres.

oxygen isotope composition of planktic and benthic foraminifera, and benthic foraminiferal assemblages are used to infer changes in salinity, temperature and sea-ice conditions along the East Greenland Shelf in the vicinity of Denmark Strait. The complete foraminiferal biostratigraphy for the cores is presented in Hansen (1998). This paper presents data from only two key benthic species.

Physical setting

The main circulation elements in the Arctic Ocean are the Beaufort Gyre and the Transpolar Drift Stream (TDS). The TDS feeds into the East Greenland Current (EGC) at Fram Strait. The EGC transports cold, low-salinity polar water (PW) and underlying Atlantic intermediate water (AIW) southward along the East Greenland margin (Aagaard and Coachman, 1968a; 1968b; Johannessen, 1986) (Figure 1). The course of the EGC coincides with the distribution of the polar pack ice and fresh water released from the Arctic Ocean. The surface currents are driven by the atmospheric circulation which is influenced in turn by the distribution of sea ice, land ice and water masses (Deser *et al.*, 2000; Rodwell *et al.*, 1999). The atmosphere directly influences sea-ice anomalies through wind-driven ice drift, and by advection of warm air toward the ice edge (Deser *et al.*, 2000). Variations in the positions and sizes of the Beaufort Gyre and the TDS are thought to influence the volumes of polar surface water and sea ice that move through the two main outflows, the Arctic Island Channels and Fram Strait (Dyke *et al.*, 1997; Tremblay *et al.*, 1997). At the other extreme, warm and saline Atlantic water flows northward in surface currents into the Nordic Seas where it cools and mixes with the polar water and eventually returns to the south along the East Greenland margin at intermediate depths (Figure 1) (Hopkins, 1991). The Atlantic intermediate water which flows through the Denmark Strait in the EGC forms part of the North Atlantic deep water (NADW), thus linking the Nordic Seas with the global thermohaline circulation.

Polar water and sea ice can advance beyond their normal limits in the EGC to bring the cold, low-salinity polar waters into the East Iceland Current (EIC). A modern example of such an event is the severe sea-ice interval in the late 1960s termed the Great Salinity Anomaly (GSA) (Malmberg, 1969; Dickson *et al.*, 1988; 1996; Mysak and Power, 1991; Serreze *et al.*, 1992). Under the influence of northerly winds, the polar water and sea ice advanced and lowered the surface salinity of the East Iceland Current to 34.7‰ such that it was effectively stratified and sea ice could form *in situ*. Dramatic changes in sea-ice distribution coincided with the GSA (Sigtryggsson, 1972). The GSA sprang from the large change in sea-ice flux through Fram Strait in 1968 (e.g., Serreze *et al.*, 1992). The most severe sea-ice years along the East Greenland and Iceland coasts have a similar pattern, with the sea ice moving into the EIC and advancing around the eastern coast of Iceland in the spring, and pushing the marine polar front southward (e.g., Sigtryggsson, 1972; Lamb, 1979). It has been proposed that the period of frequent sea-ice incidence around Iceland between 1780 and 1920 is associated with common 'GSA-like' Arctic sea-ice events (Lamb, 1979; Jennings and Weiner, 1996; Jennings *et al.*, 2001).

The Nansen Trough is a 400–500 m deep extension of the Nansen Fjord onto the inner East Greenland Shelf. The shelf is influenced both by land-fast sea ice and drifting pack ice for much of the year (Hastings, 1960). The land-fast, first-year ice usually clears by early June and forms again in November, but the offshore pack ice persists longer, with a short ice-free window in late September/early October. Polar surface water ($\leq$0°C; $\leq$34.5‰) forms the upper *c.* 150 m of the water column, and is underlain by the warmer and more saline Atlantic intermediate water ($>$0°C; $>$34.5‰). Icebergs calved from outlet glaciers of the Greenland Ice Sheet and from smaller alpine glaciers along the fjords and outer coast drift southwards in the EGC unless they become grounded on the shallow intertrough areas of the shelf (Dwyer, 1993).

The bedrock geology of the adjacent coastal area, the Blosseville Kyst, is dominated by Palaeogene flood basalts with lesser outcrops of Cretaceous-Palaeogene sedimentary strata, which include calcareous marine mudstones (Larsen *et al.*, 1999). Glacial erosion of the calcareous mudstones would provide a distinct marker of changes in iceberg-rafting from Christian IV Glacier, whereas the flood basalt is very common along most of the fjords between Scoresby Sund and Kangerlussuaq Fjord (Larsen *et al.*, 1999).

Materials and methods

The sediment cores used in this study were collected during a joint University of Tromsø/University of Colorado cruise in October 1996 on the Norwegian research vessel *Jan Mayen.* Cores JM96-1206/1-GC (68°06.0′N, 29°25.5′W; 402 m) and JM96-1207/1-GC (68°06.0′N, 29°21′W; 404 m) were raised from the Nansen Trough, a shelf-continuation of Nansen Fjord (Figure 1). The whole-round cores were logged for volume magnetic susceptibility at 5 cm intervals. The cores were split in half longitudinally, photographed and visually described. Samples, 2 cm thick, were taken from the cores every 2 cm, such that the entire working half was consumed except for a thin rind of sediment adjacent to the core liner. Benthic and planktic foraminiferal assemblages were analysed in core 1206 (at 10 cm intervals; i.e., multicentury resolution) and core 1207 (at 2 cm intervals in the upper 20 cm; i.e., 100-yr resolution, and at 10 cm intervals below 20 cm; i.e., multicentury resolution) as part of a Masters thesis (Hansen, 1998). Stable oxygen isotope analysis of the planktic foraminifer *Neogloboquadrinapachyderma* sinistral and the epifaunal benthic foraminifer *Cibicides lobatulus* were made at the Leibniz-Laboratory for Radiometric Dating and Stable Isotope Research, Kiel University, Germany. JM96-1207/1-GC is stored at INSTAAR and JM96-1206/1-GC is stored at the University of Tromsø.

IRD was quantified by counting the >2 mm clasts on x-radiographs. Clasts were counted within a 2 × 10 cm window every 2 cm. At the INSTAAR Sedimentology Laboratory, calcium carbonate content was measured by coulometer every 2 cm (*c.* 100 cal. yr). Bulk sediment samples of the <2 mm sediment were ground to a powder to homogenize the material, and small representative samples were analysed. The calcium carbonate percentages were converted to carbonate flux using the dry bulk density and the radiocarbon age model. The root mean squares error on the carbonate flux amounted to 5.1%. In JM96-1207, the >1 mm and 250 μm to 1 mm size fractions isolated during foraminiferal analyses were examined under a reflected light microscope to explore for an ice-rafted source of calcium carbonate.

Chronology

The core chronologies are based upon accelerator mass spectrometry (AMS) radiocarbon dates on foraminifera and molluscs (Table 1). The dates have been previously reported in Smith and Licht (2000) and Hansen (1998). A marine reservoir correction of 550 years was used for all of the dates (Hjort, 1973). The dates were converted to siderial years using the computer program Calib 4.1 (Stuiver *et al.*, 1998). Prior to calculation of the age models for JM96-1206 and -1207, a computer program, Analyseries (Paillard *et al.*, 1996), was used to make an independent correlation of the cores based on their volume magnetic susceptibility profiles (Figure 2). JM96-1207 was used as the reference core, because it had better dating control than core 1206 and because stratigraphic evidence shows that it represents a longer time period; glaciomarine pebbly mud forms the basal unit of JM96-1207, indicating that this core extends into the last phases of deglaciation, whereas core 1206 ended above the deglacial sediment unit. The end result of the Analyseries core-correlation process was expression of the sample depths in JM96-1206 in terms of depths in JM96-1207

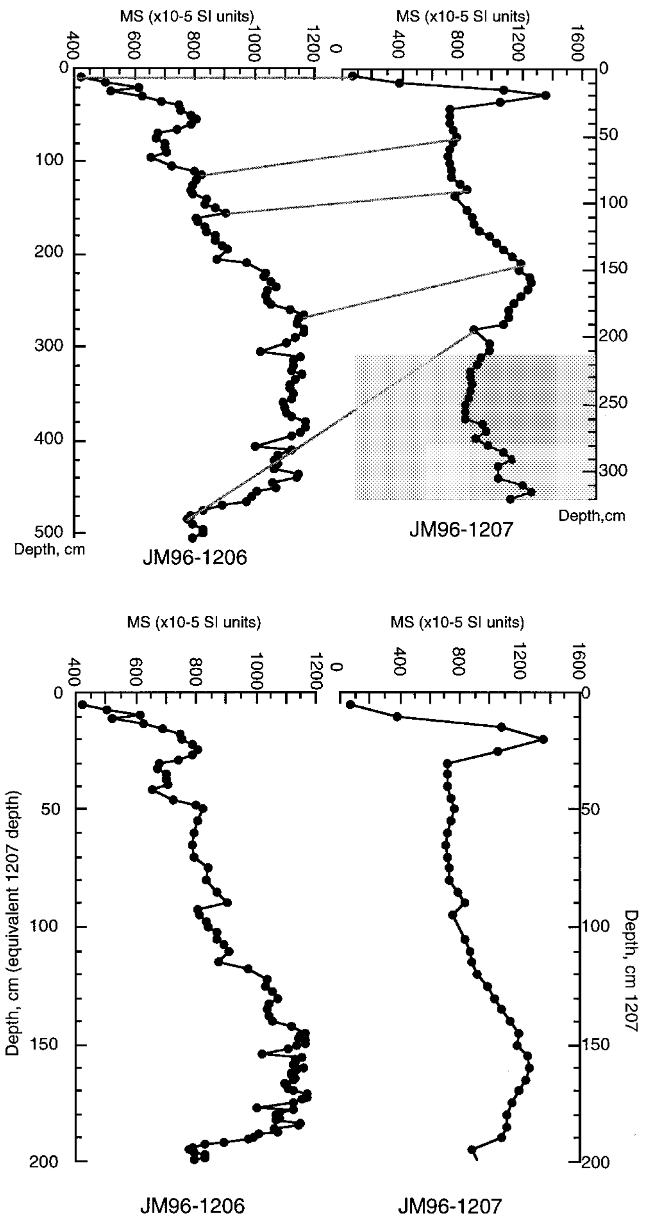

Figure 2 Top: volume magnetic susceptibility (MS) data from JM96-1206 and -1207, and correlation points used in the correlation program Analyseries (Paillard *et al.*, 1996). The grey region in JM96-1207 represents the glaciomarine sediments sampled in JM96-1207, which were beyond the reach of JM96-1206. Bottom: MS downcore data showing the resulting Analyseries correlation of the two cores, with MS in core 1206 plotted against equivalent depths in core 1207.

Table 1 Radiocarbon ages for JM96-1206-1GC and JM96-1207/1-GC

Core name	Laboratory number	Depth (cm)	Equivalent depth, 1207	Reported age	Reservoir corrected age	Calibrated mean age with 1-sigma range rounded to nearest 10		Material dated
JM96-1207	AA-24839	12–14		1575 ± 45	1025 ± 45	1000 (960)	920	Bivalve molluscs
JM96-1207	AA-23218	125–126		6210 ± 55	5660 ± 55	6540 (6470)	6400	*Arca glacialis*
JM96-1207	AA-24840	160–162		8250 ± 60	7700 ± 60	8620 (8560)	8470	Bivalve fragments
JM96-1207	CAMS-32047	324		9800 ± 60	9250 ± 60	10580 (10310)	10270	Benthic foraminifers
JM96-1206	AAR-4560	50–52	22.14	2185 ± 50	1635 ± 50	1680 (1590)	1530	Benthic foraminifers
JM96-1206	AAR-4561	180–182	102.5	4990 ± 60	4440 ± 60	5280 (5210)	5040	Benthic foraminifers
JM96-1206	Tua-1926	400–402	176	9735 ± 120*	9185 ± 120*	10570 (10300)	10150	*C. neoteretis*

*Age considered to be too old based on foraminiferal stratigraphy (Hansen, 1998).

(Figure 2). Using this common depth scale, the calibrated radiocarbon dates from both cores were together used to determine the age model, and depths in the cores were converted to cal. age BP (Figure 3). The date at 400 cm in 1206 was excluded from the age model because it was considered to be too old (i.e., reworked) based on comparison of the foraminiferal stratigraphies of the two cores (Hansen, 1998). The age model is comprised of two linear equations. There is a large change in sedimentation rate associated with the lithofacies boundary between marine mud and glaciomarine pebbly mud in JM96-1207, which occurs at 214 cm. The upper linear segment is extended to 200 cm, the extent of the correlation between JM96-1206 and JM96-1207, and ages from the core top to 200 cm are expressed as: age cal. yrs = 338.06 + 49.747x, where x is the central depth of the sample interval, and $R^2 = 0.996$ (Figure 3). The ages of samples below 200 cm and within the glaciomarine pebbly mud were determined by: age cal. yrs = 10 251 + 0.182x, where x is the central depth of the sample interval (Figure 3). Although it would appear to be logical to extend the upper linear age model to the lithofacies boundary at 214 cm, doing so created an age inversion with the radiocarbon date below, in the glaciomarine pebbly mud. Lacking a radiocarbon date at the lithofacies boundary, we chose 200 cm as the inflection point between the two linear segments (Figure 3).

Results

Ice-rafted detritus (IRD)

Both cores are comprised of homogeneous dark grey and brownish grey silty clay with scattered sand and gravel grains. This lithofacies is the common postglacial Holocene lithological unit on the East Greenland Shelf in the vicinity of the Denmark Strait (e.g., Smith, 1997; Andrews *et al.*, 1997; Williams *et al.*, 1995b). Core JM96-1207 extends through this upper unit into stiff pebbly mud at 214 cm (*c*. 10.9 cal. ka). The stiff pebbly mud is interpreted to represent distal glaciomarine sediments. The high IRD contents in the glaciomarine pebbly mud reflect iceberg-rafting during the final phases of deglaciation when glacier ice retreated into the fjords. The postglacial IRD contents of JM96-1206 and JM96-1207 are quite low until *c*. 5 cal. ka. Terrestrial glacier mapping indicates that glacier ice margins had retreated to positions behind their present margins by 7 ka (Funder, 1989; Geirsdóttir *et al.*, 2000). The low IRD contents over this interval probably reflect a combination of ice fronts terminating on land rather than in tidewater, and warm conditions in which IRD would be melted out in the fjords. However, there was a very low influx of IRD throughout the interval.

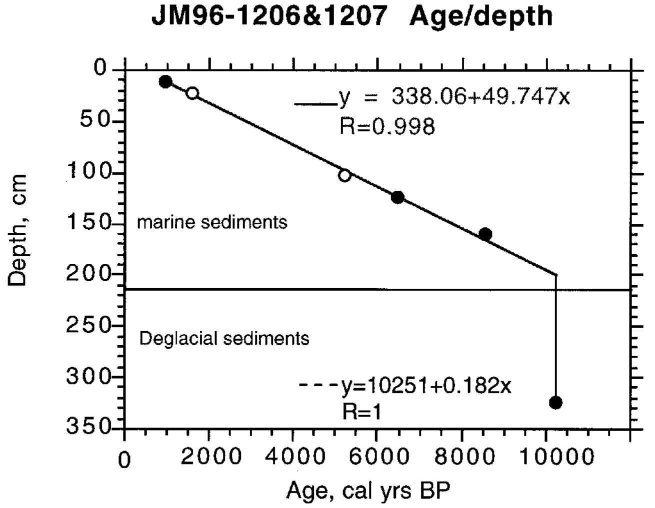

Figure 3 Age-depth plot showing age model for combined cores JM96-1206 and -1207 based on Analyseries correlation of the two, shown in Figure 2. The postglacial marine sediments were deposited at a slower rate than the deglacial sediments (glaciomarine pebbly mud). Open circles represent dates from JM96-1206 and filled circles represent dates from JM96-1207. Table 1 lists the 1-sigma ranges on the calibrated ages. These age ranges generally are contained within the size of the dot that symbolizes each date.

IRD contents increase between 5 and 4.5 cal. ka BP in the Nansen Trough (Figure 4). Specific peaks and troughs in the >2 mm counts do not compare one-to-one, but the overall trends of increasing IRD in the last 5 cal. ka are similar. We interpret this increase in IRD content to reflect climatic cooling, which is consistent with advance of glaciers into tidewater to greatly increase iceberg-rafting. Once iceberg-rafting was occurring, the sea surface had to be cold for the icebergs to retain their debris on the shelf instead of releasing it during transit of the fjords (Syvitski *et al.*, 1996). Atmospheric cooling (i.e., decreasing $\delta^{18}O$ ratios) after 4.7 cal. ka BP in the Renland ice core (Johnsen *et al.*, 1992) and decreasing summer insolation at 60°N throughout the Holocene (Berger and Loutre, 1991) support the interpretation of cooling (Figure 4). The overall pattern of IRD seen in the JM96 cores from Nansen Trough is similar to the IRD record from Nansen Trough core BS1191-K15 (Figure 4) and other cores from the East Greenland shelf (Andrews *et al.*, 1997), supporting the broad millennial interpretations of early-Holocene warmth changing to later-Holocene cooling after *c*. 5 cal. ka.

Stable isotopes and foraminifera

In JM96-1207, light $\delta^{18}O$ spikes and generally variable $\delta^{18}O$ values occur in the glacial-marine sediments below 214 cm (10.9 cal. ka) (Figure 5). The light values are interpreted to reflect isotopically light glacial meltwater associated with the final stages of deglaciation. Relatively high percentages of *Elphidium excavatum* f. *clavata* coincide with the distal glacial-marine sediments, substantiating the interpretation of reduced salinities such as would typify a glacier-influenced environment (Hald *et al.*, 1994).

The $\delta^{18}O$ compositions of the planktic foraminifer *N. pachyderma* sinistral and the benthic foraminifer *C. lobatulus* become progressively lighter after the end of deglaciation throughout the rest of the Holocene. We attribute the early phases of the $\delta^{18}O$ lightening to warming, although as much as 0.2–0.3‰ of this change can be attributed to continued eustatic sea-level rise until *c*. 7 cal. ka (Fairbanks, 1989). Warming cannot easily explain the continued decrease in the $\delta^{18}O$ in the later half of the Holocene, given the external evidence for cooling in the Renland ice core $\delta^{18}O$ and the decreasing solar insolation (Figure 5). Therefore, we interpret the continued depletion in $\delta^{18}O$ of the last *c*. 5 cal. ka to freshening of the water column. A pronounced peak in *Elphidium excavatum* f. *clavata* percentages at 6 cal. ka in JM96-1206 is not resolved in JM96-1207, but may be significant (Figure 5). Freshening appears to have been especially pronounced during the last 2 cal. ka with increasing percentages of *E. excavatum* f. *clavata* and more strongly decreasing planktic $\delta^{18}O$ values (Figure 5).

Coherent changes in planktic and benthic $\delta^{18}O$ records occur throughout the Holocene. This result is not unexpected, given that *N. pachyderma* sinistral probably lives close to the transition between AIW and surface polar water (e.g., Pflaumann *et al.*, 1996; Kohfeld *et al.*, 1996; Ostermann *et al.*, 1998), and as the AIW continues to the sea floor in Nansen Trough. The similar depletion in $\delta^{18}O$ values in the planktic and benthic records suggests a process that affected the entire water column. Increased freshening of the sea surface stratifies the water column and isolates the sea bed from the sea surface. However, *in situ* sea-ice formation may produce brines that could carry the light isotopic signal to the sea floor (Dokken and Jansen, 1999). The rise in *Elphidium excavatum* f. *clavata* over the last 5 cal. ka provides independent evidence of an overall freshening of the water

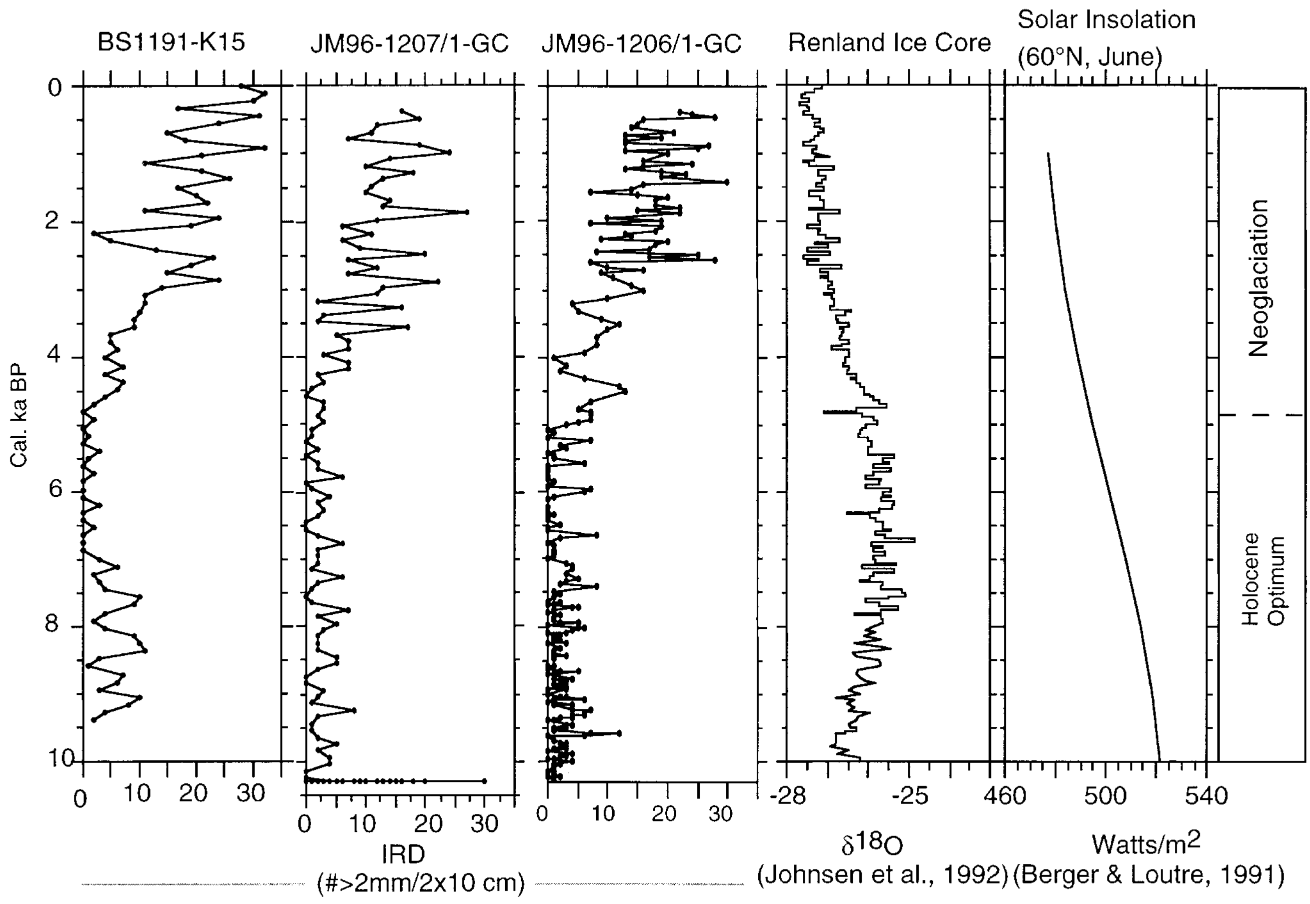

Figure 4 IRD records from cores from the Nansen Trough against the Renland $\delta^{18}O$ (Johnsen *et al.*, 1992) record and the solar insolation at 60°N (Berger and Loutre, 1991). IRD data from BS1191-K15 are from Andrews *et al.* (1997).

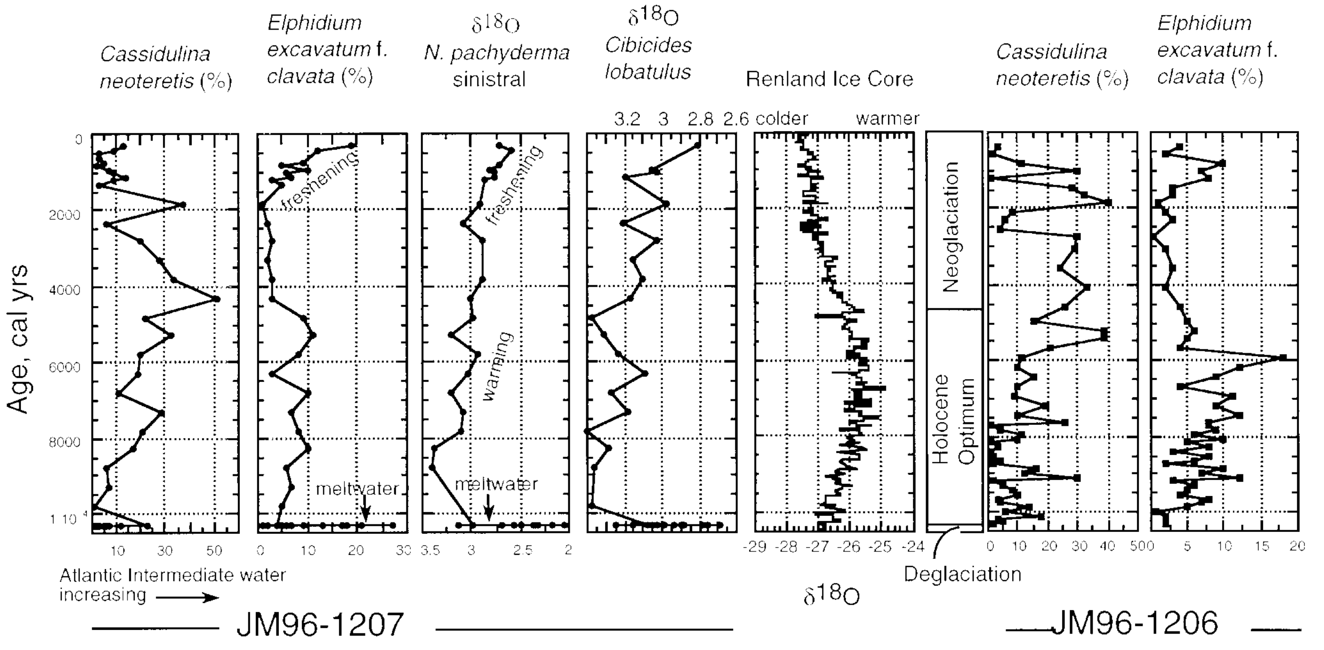

Figure 5 Foraminiferal and stable isotope data for JM96-1207 and foraminiferal data from JM96-1206 against the Renland $\delta^{18}O$ record.

column, especially during the last 2 cal. ka. We suggest that an increase in PW during this period affected the AIW towards lighter $\delta^{18}O$, by increasing the relative proportion of PW mixed in the AIW. This mixing can occur by various mechanisms, such as thermohaline convection and brine formation, but the data presented cannot resolve the cause of the depletion in the $\delta^{18}O$ values.

Trends in the percentages of *Cassidulina neoteretis*, an indicator of relatively warm Atlantic intermediate water (Jennings and Weiner, 1996; Jennings and Helgadottir, 1994), of the EGC, increase during the early Holocene in both cores and reach maximum percentages of between 40 and 50 % in the middle Holocene. This trend is consistent with the other indicators of relatively warm conditions after deglaciation until *c.* 5 cal. ka

(Figure 5). *C. neoteretis* percentages diminish gradually after 4.5 cal. ka in JM96-1207, but remain between 25 and 30% in JM96-1206 until *c*. 2.7 cal. ka before diminishing to values below 10 %. Between *c*. 2 and 1.5 cal. ka, *C. neoteretis* rises again to percentage peaks in both cores. This interval of high percentages of *C. neoteretis* coincides with abundance peaks in both the planktic and benthic foraminifers (Hansen, 1998). The *C. neoteretis* peak between *c*. 2 and 1.5 cal. ka suggests an interval of diminished sea ice and stronger influence of Atlantic intermediate water on the East Greenland Shelf at this time (Hansen, 1998).

Carbonate flux, a new proxy for IRD on the East Greenland Shelf

Calcium carbonate (TIC) contents vary between 0 and 6% in JM96-1207, although most samples have values of less than 2%. The glaciomarine pebbly mud has higher calcium carbonate percentages overall than the overlying postglacial marine mud has. Calcium carbonate fluxes in JM96-1207 calculated at 100-yr spacing reveal small but pronounced peaks (Figure 6). There is a change in the regularity and spacing of the carbonate flux peaks at *c*. 4.7 cal. ka, coinciding very closely with the 4.7 cal. ka onset of Neoglacial cooling in the Renland ice core δ^{18}O record. After 4.7 cal. ka, the carbonate peaks are regularly spaced and uniform in magnitude. Below 4.7 cal. ka, they are irregular in magnitude and spacing. There are six detrital carbonate flux peaks and five detrital carbonate troughs between 4.7 and 0.4 cal. ka (Figure 6).

We compared the carbonate record from JM96-1207 with the GISP2 record of sea salt sodium (Na) flux (Figure 6). Increases in sea salt Na flux have been interpreted to indicate windier, colder, drier climatic intervals (O'Brien *et al*., 1995). In most cases, the carbonate peaks after 4.7 cal. ka correspond with increases in sea salt Na flux (i.e., coolings), but, prior to the 4.7 cal. ka shift, the association between sea salt Na flux and carbonate peaks is less clear. For example, below the shift, two of the major sea salt high flux intervals correspond in general with carbonate lows, but otherwise the pattern is inconsistent (Figure 6).

The origin of the carbonate is important to the interpretation of the carbonate peaks. Foraminiferal carbonate is one source of carbonate in the cores. However, comparison of the foraminiferal concentration (foraminifers/100 g sediment) with the carbonate flux shows no relation between the carbonate flux peaks and foraminiferal concentration (Figure 7). Another source of carbonate was observed in the >1 mm and >250 μm fractions of the core. Calcareous tan siltstone fragments and quartz sandstone fragments with calcite cement were identified under the stereomicroscope, especially in the high calcium carbonate flux intervals of the last 4.7 cal. ka and in the deglacial sediments (glaciomarine pebbly mud). These grains are likely to be derived from glacial erosion of the calcareous Cretaceous mudstones that outcrop along the drainage basin of the Christian IV Glacier and the adjacent Sorgenfri Glacier, and possibly sedimentary basins farther to the north near Scoresby Sund (Larsen *et al*., 1999). Basaltic grains dominated the >2 mm fractions, and no siltstones were observed, suggesting that glacial erosion of the softer Cretaceous sedimentary units does not generally produce clasts larger than 2 mm, the size of IRD that is counted on the x-radiographs (Andrews, 2000). Given the absence of a correlation between foraminiferal content and total carbonate, glacial erosion of the calcareous Cretaceous

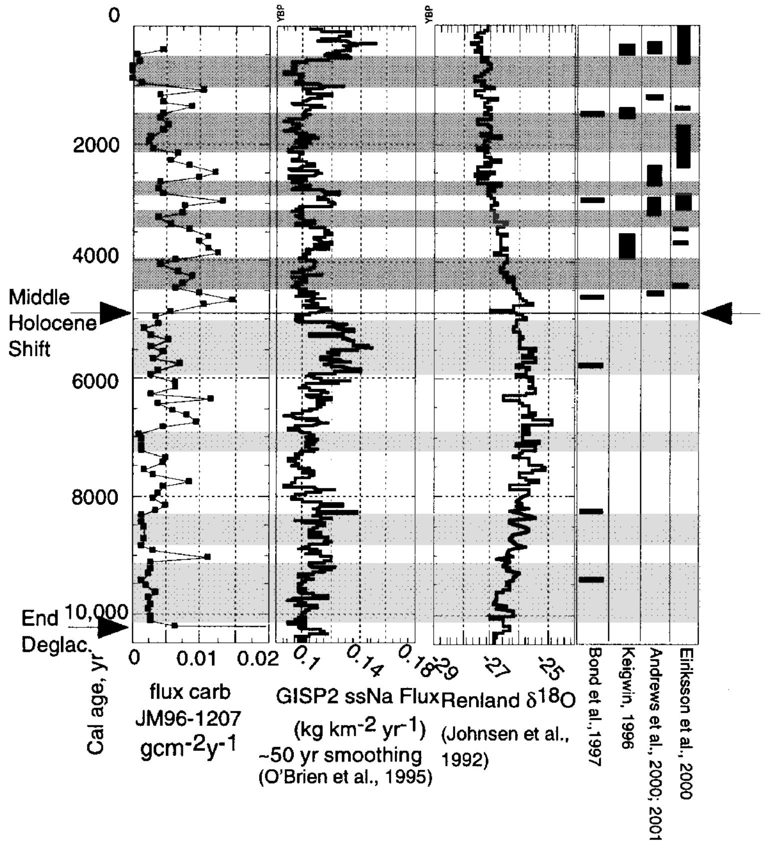

Figure 6 Detrital carbonate flux data from JM96-1207 against GISP2 sea salt Na flux (O'Brien *et al*., 1995) and the Renland δ^{18}O record (Johnsen *et al*., 1992). The carbonate flux peaks above the mid-Holocene shift *c*. 4.7 cal. ka are interpreted as sea-surface coolings and are demarcated as white areas. These carbonate flux peaks correspond with peaks in sea salt Na flux and with sea-surface coolings recorded in cores off Ireland (Bond *et al*., 1997), Iceland (Andrews *et al*., 2000; Eiriksson *et al*., 2000), and on the Bermuda rise (Keigwin, 1996). Below the mid-Holocene shift, intervals of low carbonate flux in JM96-1207 correspond with intervals of elevated sea salt Na flux, and the carbonate flux peaks do not correspond to coolings.

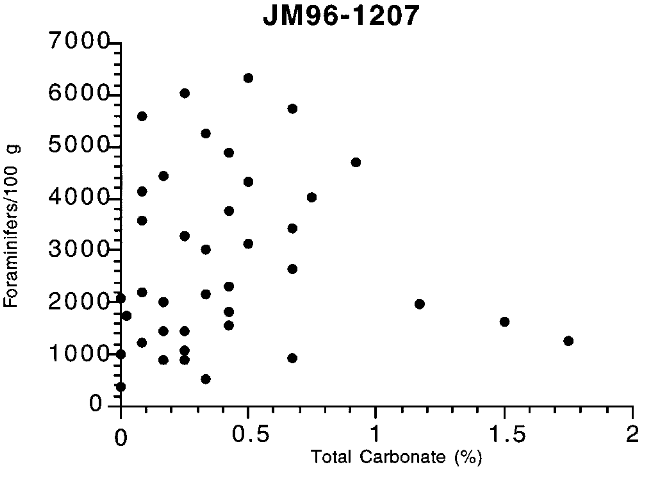

Figure 7 Scatterplot of the total carbonate percentage data from levels in core JM96-1207 that also have foraminiferal concentration data (Hansen, 1998). There is no correlation between these two measures of carbonate content.

mudstone and possibly other facies of the Cretaceous-Paleogene sediments, especially by the Christian IV Glacier that drains into the head of Nansen Fjord, is considered to be the dominant source of the carbonate flux peaks.

Causes of Neoglacial cooling and significance of the carbonate flux peaks

A general pattern of early- to mid-Holocene warm conditions followed by Neoglacial cooling is recognized throughout the Arctic areas of the North Atlantic (e.g., Nesje and Dahl, 1993; Koç *et al.*, 1993; Williams *et al.*, 1995a). The causes of Neoglacial cooling are not well constrained. Postglacial emergence of the Arctic Island Channels has been invoked as a possible explanation (Williams *et al.*, 1995a). As these channels rose above the level of the Atlantic layer in the Arctic Ocean, the warmer saltier water was excluded from the outflow and dramatically changed the character of the Baffin Current and the Labrador Current (e.g., Osterman and Nelson, 1989; Jennings, 1993). Such a change in the bathymetry of the Arctic Island Channels would affect Baffin Bay, but the outflow of water from the Arctic Ocean through the Fram Strait has not been impeded by bathymetric changes. Decreased solar insolation beyond a critical threshold and preferred atmospheric circulation pattern such as northerly winds and NAO (North Atlantic Oscillation) indices have been presented as possible causes for Neoglacial cooling (Andrews *et al.*, 1997; Keigwin and Pickart, 1999; Koç and Jansen, 1994; Williams *et al.*, 1995a). The data from the East Greenland Shelf are consistent with Neoglacial cooling forced by decreased solar insolation beyond a critical threshold and enhanced by a resultant advance of the southern margin of the Arctic drift ice along the East Greenland margin as suggested by Koç *et al.* (1993) and Koç and Jansen (1994) for the Nordic Seas.

The shift in the association between the carbonate flux and the sea salt Na flux reflect the influence of Neoglacial cooling on glacier margins. The IRD records in this study and in Andrews *et al.* (1997) and the glacial geologic record (Funder, 1989) indicate that East Greenland glaciers advanced into tidewater sometime between 6 and 4 cal. ka. Advance of the Christian IV Glacier into Nansen Fjord would initiate delivery of Cretaceous calcareous mudstone bedrock that crops out in the drainage basin. Although Neoglacial ice fluctuations may be significant and rapid (cf. Geirsdóttir *et al.*, 2000; Karlén, 1988), they are poorly known in the region, especially for the early Neoglacial interval. We suggest that the carbonate flux peaks are more closely related to sea-surface cooling (or enhanced polar water flux) than to specific glacier oscillations, because of the rapidity of the changes, but glacier oscillations cannot be ruled out as the cause of the carbonate flux peaks.

Under conditions of increased polar water flux along East Greenland, icebergs calved in the fjords would retain their debris farther onto the shelf (where it would be recorded in JM96-1207), rather than lose their debris to melting within the fjords, especially if the icebergs were not trapped in permanent sikussaq at the glacier margin (Syvitski *et al.*, 1996). Such a pattern of sensitivity of iceberg melt and debris distribution has been suggested by Dowdeswell *et al.* (2000) for both Nansen Fjord and Scoresby Sund. We suggest that the carbonate peaks reflect advances of the polar front during the Neoglacial interval, associated with strengthening of the EGC and increased deposition of calcareous mudstone IRD on the shelf.

Neoglacial sea-surface coolings of similar ages to the carbonate flux peaks in Nansen Trough have been interpreted from deep-sea cores (Figure 6). Keigwin (1996) interpreted a 1°C cooling during the 'Little Ice Age' and during a similar event *c.* 1500 years ago, and a warming of 1°C during the 'Medieval Warm Period'. He recognized another cool interval associated with increased ice-rafted debris beginning between 4 and 5 ka, suggesting that this event marks the beginning of Neoglacial cooling. Bond *et al.* (1997) documented millennial scale coolings throughout the Holocene in two cores off Ireland (VM 29–191 and VM 23–81). The Holocene cool intervals are manifested by ice-rafting (hematite-coated grains) and increased abundances of *N. pachyderma* sinistral at 1.5, 3.0, 4.5, 5.8, 8.2 and 9.5 cal. ka. Bond *et al.* (1997) argue that there is a 1470 ± 500-year cycle to these events that occurs unbroken through the Holocene and beyond. Giraudeau *et al.* (2000) interpret sea-surface instabilities (EH events denoted by variations in the coccolith *Emiliani huxleyi*) correlative to Bond *et al.*'s (1997) events in a core from the Gardar Drift. They attribute the EH events younger than *c.* 6 ka to closer proximity of the subpolar front in response to decreasing solar insolation. However, they attribute the 8.2 ka EH event to meltwater from the Laurentide Ice Sheet (Barber *et al.*, 1999).

The sea-surface coolings interpreted in East Greenland core JM96-1207 correspond with cooling events in the deep sea, but additional peaks centred around 2.4 and 3.8 cal. ka were also resolved, suggesting that the shelf site captures higher-frequency events which may not be recorded in the deep-sea records (Figure 6). Given their positions well away from the direct influence of the sea ice, the deep-sea cores may record only the most extreme periods of sea-ice excursion, whereas the Nansen Trough cores may record less severe events. The Nansen Trough record suggests that the coolings occur more frequently than was proposed by Bond *et al.* (1997).

Several Neoglacial sea-surface coolings have been reconstructed on the Northern Iceland shelf. The coolings are inferred from calcium carbonate (coccoliths) flux changes reflecting changes in sea-surface primary productivity (Andrews *et al.*, 2000; 2001), and variations in the percentages of *N. pachyderma* sinistral and IRD variations (Eiriksson *et al.*, 2000). Once again, these coolings appear to coincide fairly closely with the Nansen Trough cool periods and with the other Neoglacial age coolings noted in the deep-sea records from the North Atlantic (Figure 6).

The appearance of IRD in East Greenland records between 6 and 4 cal. ka BP, and the onset of the detrital carbonate flux peaks *c.* 4.7 cal. ka, suggest that severe Arctic sea-ice events began in the Neoglacial interval, and that earlier-Holocene cool events in the deep-sea records are associated with different processes, for example the catastrophic drainage of glacial lake Ojibway-Barlow at 8.2 cal. ka (Barber *et al.*, 1999). However, it cannot be denied that the detrital carbonate proxy can only be active when glaciers have advanced into tidewater such that calving of icebergs could occur. For example, a strong cooling recorded by Bond *et al.* (1997) *c.* 5.8 ka may be reflected by the peak in *Elphidium excavatum* f. *clavata* recorded in JM96-1206 *c.* 5.8 cal. ka BP, but the IRD and carbonate proxies do not record this event, because the glaciers had not yet advanced into tidewater. Evidence across the North Atlantic region suggests that the southern margin of the Arctic sea ice was well north of its current position in the early Holocene (Koç *et al.*, 1993), so that sea-ice propagated coolings beginning *c.* 5.8 cal. ka are reasonable, but early-Holocene coolings, such as the 8.2 cal. ka event, are more likely forced by other mechanisms (e.g., Barber *et al.*, 1999).

We suggest that the Neoglacial age North Atlantic sea-surface coolings are related to periods of increased sea-ice extent. This mechanism unifies the observations of sea-surface coolings off East Greenland and Northern Iceland, and in the North Atlantic. However, the causes of decadal to century-scale variability in sea-ice extent are not well known. The periods of increased sea-ice extent are probably linked with increased freshwater and sea-ice fluxes from the Arctic Ocean through Fram Strait. For example, there is a strong correlation between positive phases of the North Atlantic Oscillation (NAO) (Hurrell, 1995) and winter sea-ice flux through Fram Strait, but the correlation is reduced during negative NAO years (Kwok and Rothrock, 1999). A positive NAO index is associated with strong sea-level pressure gradients across Fram Strait, resulting in strong winds that enhance ice export through both Fram Strait and the Denmark Strait; these large-scale atmospheric patterns break down during the negative NAO years, reducing the correlation between ice flux and NAO (Kwok and Rothrock, 1999). Deser *et al.* (2000) point out that the correlation between NAO and sea-ice anomalies is imperfect in detail and that local influences on the sea-ice distribution are important. An extreme example of the lack of correlation between the NAO and the sea-ice flux is the Great Salinity Anomaly. The late 1960s are characterized by negative NAO indices, yet the Great Salinity Anomaly occurred during this time period, indicating that atmospheric circulation patterns described by strongly negative NAO indices can also result in large positive sea-ice anomalies. The association of ice flux through Fram Strait with both positive and extreme negative NAO states has been termed the GSA paradox by Dickson *et al.* (2000). In addition, conditions favouring export of thicker, lower-salinity multiyear ice through the Fram Strait may play an important role in forming positive sea-ice and salinity anomalies south of Fram Strait (Mysak and Power, 1991; Tremblay *et al.*, 1997; Rothrock *et al.*, 2000).

Documentary data have shown that in the past few centuries there have been prolonged periods of greater sea-ice extent, on average, in the Nordic Seas than occurs at present (e.g., Ogilvie, 1984). The proxy evidence from the Nansen Trough suggests that these prolonged periods of greater sea-ice incidence have occurred at intervals throughout the last 5 ky. Continued efforts to understand the atmospheric/ocean interactions that result in sea-ice variability on annual, decadal and century timescales are needed to explain the natural variability that is observed in Holocene records of sea-surface conditions in the Nordic Seas.

Conclusions

(1) The transition from distal glacial-marine to postglacial marine sedimentation began the Nansen Trough *c.* 10.9 cal. ka.

(2) Holocene conditions in the Nansen Trough between 10.9 cal. ka and *c.* 4.7 cal. ka were little influenced by glacier ice and indicate a dominant influence of Atlantic intermediate water in the EGC. The low IRD content of the sediments indicates either that most ice margins had retreated out of the marine environment or that most icebergs melted in the fjords. Foraminiferal faunas were dominated by *C. neoteretis*, a consistent indicator of Atlantic intermediate water.

(3) Neoglacial cooling became evident in the Nansen Trough *c.* 4.7 cal. ka. It was associated with southward expansion of the Arctic sea ice and increased polar water influence in the EGC. Carbonate flux peaks in the Nansen Trough reflect iceberg rafting of Cretaceous calcareous mudstone clasts onto the shelf.

(4) Freshening of the EGC was pronounced after 2 cal. ka.

(5) Cooling and warming cycles interpreted from the carbonate flux variations may indicate multiple warming and cooling cycles similar to the so-called ‘Little Ice Age’ and ‘Medieval Warm Period’ type cycles of greater and lesser sea-ice extent throughout the Neoglacial interval.

Acknowledgements

The research was supported by National Science Foundation grant OPP-9707161. We appreciated the thorough reviews by N. Koç and an anonymous reviewer. Thanks are due the scientific party and the personnel of *Jan Mayen* for their help in sampling the cores.

References

Aagaard, K. and **Carmack, E.C.** 1994: The Arctic Ocean and climate: a perspective. In *The polar oceans and their role in shaping the global environment*, Geophysical Monograph 85, American Geophysical Union, 5–20.

Aagaard, K. and **Coachman, L.K.** 1968a: The East Greenland Current north of Denmark Strait: Part I. *Arctic* 21, 181–200.

—— 1968b: The East Greenland Current north of Denmark Strait: Part II. *Arctic* 21, 267–90.

Aagaard, K., Fahrbach, E., Meincke, J. and **Swift, J.H.** 1991: Saline outflow from the Arctic Ocean: its contribution to the deep waters of the Greenland, Norwegian, and Iceland Seas. *Journal of Geophysical Research* 96(C11), 20433–41.

Andrews, J.T. 2000: Icebergs and iceberg rafted detritus (IRD) in the North Atlantic: facts and assumptions. *Oceanography* 13, 100–108.

Andrews, J.T., Helgadottir, G., Geirsdóttir, A., Hardardottir, J., Kristjansdottir, G., Smith, L.M., Jennings, A.E. and **Sveinbjornsdottir, A.** 2000: The carbonate content of cores on the N Iceland shelf: high-resolution records for the last 5 ka of surface productivity and sea-ice. In CAPE/ICAPP Abstracts: sea ice in the climate system, the record of the North Atlantic Arctic, 2–6 June 2000, Kirkjubaejarklaustur, Iceland.

Andrews, J.T., Helgadottir, G., Geirsdóttir, A. and **Jennings, A.E.** 2001: 4800 years of high-resolution records of ocean productivity (?) changes off N. Iceland: the Little Ice Age in perspective. *Quaternary Research*, in press.

Andrews, J.T., Smith, L.M., Preston, R., Cooper, T. and **Jennings, A.E.** 1997: Spatial and temporal patterns of iceberg rafting (IRD) along the East Greenland margin, ca. 68°N, over the last 14 cal. ka. *Journal of Quaternary Science* 12, 1–13.

Barber, D.C., Dyke, A., Hillaire-Marcel, C., Jennings, A.E., Andrews, J.T., Kerwin, M.W., Bilodeau, G., McNeely, R., Southon, J., Moorehead, M.D. and **Gagnon, J.-M.** 1999: Forcing of the cold event of 8200 years ago by catastrophic drainage of Laurentide lakes. *Nature* 400, 344–48.

Berger, A. and **Loutre, M.F.** 1991: Insolation values for the climate of the last 10 million years. *Quaternary Sciences Reviews* 10(4), 297–317.

Bond, G., Showers, W., Cheseby, M., Lotti, R., Almasi, P., deMenocal, P., Priore, P., Cullen, H., Hajdas, I. and **Bonani, G.** 1997: A pervasive millennial-scale cycle in North Atlantic Holocene and Glacial climates. *Science* 278, 1257–66.

Deser, C., Walsh, J.E. and **Timlin, M.S.** 2000. Arctic sea ice variability in the context of recent atmospheric circulation trends. *Journal of Climate* 13, 617–33.

Dickson, R.R. 1997: From the Labrador Sea to global change. *Nature* 386, 649–50.

Dickson, R.R., Lazier, J., Meincke, J., Rhines, P. and **Swift, J.** 1996: Long-term coordinated changes in the convective activity of the North Atlantic. *Progress in Oceanography* 38, 241–95.

Dickson, R.R., Meincke, J., Malmberg, S. and **Lee, A.** 1988: The 'Great Salinity Anomaly' in the Northern North Atlantic 1968–1982. *Progress in Oceanography* 20, 103–51.

Dickson, R.R., Osborn, T.J., Hurrell, J.W., Meincke, J., Blindheim, J., Adlandsvik, B., Vinje, T., Alekseev, G. and **Maslowski, W.** 2000: The Arctic Ocean response to the North Atlantic Oscillation. *Journal of Climate* 13, 2671–96.

Dokken, T.M. and **Jansen, E.** 1999: Rapid changes in the mechanism of ocean convection during the last glacial period. *Nature* 401, 458–61.

Dowdeswell, J.A., Whittington, R.J., Jennings, A.E., Andrews, J.T., Mackensen, A. and **Marienfeld, P.** 2000: An origin for laminated glacimarine sediments through sea-ice build-up and suppressed iceberg rafting. *Sedimentology* 47, 557–76.

Dwyer, J.L. 1993: Monitoring characteristics of glaciation in the Kangerlussuaq Fjord region, East Greenland, using digital LANDSAT MSS and TM data. Thesis, University of Colorado, Boulder, 202 pp.

Dyke, A.S., England, J., Reimnitz, E. and **Jette, H.** 1997: Changes in driftwood delivery to the Canadian Arctic Archipelago: the hypothesis of Postglacial oscillations of the Transpolar Drift. *Arctic* 50(1), 1–16.

Eiriksson, J., Knudsen, K.L., Haflidason, H. and **Heinemeier, J.** 2000: Chronology of late Holocene climatic events in the northern North Atlantic based on AMS ^{14}C dates and tephra markers from the volcano Hekla, Iceland. *Journal of Quaternary Science* 15, 23–42.

Fairbanks, R.G. 1989: A 17,000-year glacio-eustatic sea level record: influence of glacial melting rates on the Younger Dryas event and deep-ocean circulation. *Nature* 342, 637–42.

Funder, S. 1989: Quaternary geology of East Greenland. In Fulton, R.J., editor, *Quaternary geology of Canada and Greenland*, vol. K1, Geological Society of America, 756–63.

Geirsdóttir, A., Hardardottir, J. and **Andrews, J.T.** 2000: Late-Holocene terrestrial glacial history of Miki and I.C. Jacobsen Fjords, East Greenland. *The Holocene* 10, 123–34.

Giraudeau, J., Cremer, M., Manthé, S., Labeyrie, L. and **Bond, G.** 2000: Coccolith evidence for instabilities in surface circulation south of Iceland during Holocene times. *Earth and Planetary Science Letters* 179, 257–68.

Hald, M., Steinsund, P.I., Dokken, T., Korsun, S., Polyak, L. and **Aspeli, R.** 1994: Recent and late Quaternary distribution of *Elphidium excavatum* f. *clavatum* in arctic seas. *Cushman Foundation Special Publication* 32, 141–53.

Hansen, K.V. 1998: Holocene foraminifera stratigraphy and climatic fluctuations in the Denmark Strait, East Greenland. Thesis in Micropaleontology, Department of Marine Geology, University of Aarhus, Denmark, 85 pp.

Hastings, A.D. 1960: *Environment of Southeast Greenland*. Quartermaster Research and Engineering Command, Technical Report EP-140.

Hjort, C. 1973: A sea correction for East Greenland. *Geologiska Föreningen Stockholm Förhandlingar* 95, 132–34.

Hopkins, T.S. 1991: The GIN Sea – a synthesis of its physical oceanography and literature review 1972–1985. *Earth-Science Review* 30, 175–318.

Hurdle, B.G. 1986: *The Nordic seas*. New York: Springer-Verlag, 777 pp.

Hurrell, J.W. 1995: Decadal trends in the North Atlantic Oscillation: regional temperatures and precipitation. *Science* 269 (4 August), 676–79.

Jennings, A.E. 1993: The Quaternary history of Cumberland Sound, southeastern Baffin Island, Canada: the marine evidence. *Géographie Physique et Quaternaire* 47, 21–42.

Jennings, A.E. and **Helgadottir, G.** 1994: Foraminiferal assemblages from the fjords and shelf of Eastern Greenland. *Journal Foraminiferal Research* 24, 123–44.

Jennings, A.E. and **Weiner, N.J.** 1996: Environmental change on eastern Greenland during the last 1300 years: evidence from Foraminifera and Lithofacies in Nansen Fjord, 68°N. *The Holocene* 6, 179–91.

Jennings, A.E., Hagen, S., Hardardottir, J., Stein, R., Ogilvie, A.E.J. and **Jonsdottir, I.** 2001: Oceanographic change and terrestrial human impacts in a post A.D. 1400 sediment record from the southwest Iceland shelf. *Climatic Change* 48 (Special Issue, The Iceberg in the Mist: Northern Research in Pursuit of 'A Little Ice Age', guest editors Ogilive, A.E. and Jónsson, T.), 83–100.

Johannessen, O.M. 1986: Brief overview of the physical oceanography. In Hurdle, B.G., editor, *The Nordic seas*, New York: Springer-Verlag, 103–28.

Johnsen, S., Clausen, H.B., Dansgaard, W., Gundestrup, N.S., Hansson, M., Johnsson, P., Steffensen, P. and **Sveinbjornsdottir, A.E.** 1992. A 'deep' ice core from East Greenland. *Meddelelser om Gronland, Geoscience* 29, 22 pp.

Karlén, W. 1988: Scandinavian glacial and climatic fluxtuations during the Holocene. *Quaternary Science Reviews* 7, 199–209.

Keigwin, L.D. 1996: The Little Ice Age and Medieval Warm Period in the Sargasso Sea. *Science* 274 (29 Nov.), 1504–508.

Keigwin, L.D. and **Pickart, R.S.** 1999: Slope water current over the Laurentian Fan on interannual to millennial time scales. *Science* 286, 520–23.

Knudsen, K.L. and **Eiriksson, J.** 2001: Application of tephrochronology to the timing and correlation of palaeoceanographic events in Holocene and Lateglacial sediments off North Iceland. *Marine Geology*, in press.

Koç, N. and **Jansen, E.** 1994: Response of the high latitude northern hemisphere to orbital climate forcing: evidence from the Nordic Seas. *Geology* 22, 523–26.

Koç, N., Jansen, E. and **Haflidason, H.** 1993: Paleoceanographic reconstructions of surface ocean conditions in the Greenland, Iceland and Norwegian seas through the last 14 ka based on diatoms. *Quaternary Science Reviews* 12, 115–40.

Kohfeld, K.E., Fairbanks, R.G., Smith, S.L. and **Walsh, I.D.** 1996: *Neogloboquadrina pachyderma* (sinistral coiling) as paleoceanographic tracers in polar oceans: evidence from northeast water Polynya plankton tows, sediment traps, and surface sediments. *Paleoceanography* 11, 679–99.

Kwok, R. and **Rothrock, D.A.** 1999. Variability of Fram Strait ice flux and North Atlantic Oscillation. *Journal of Geophysical Research* 104, 5177–89.

Lamb, H.H. 1979: Climatic variation and changes in the wind and ocean circulation: the Little Ice Age in the northeast North Atlantic. *Quaternary Research* 11, 1–20.

Larsen, M., Hamberg, L., Olaussen, S., Nørgaard-Pedersen, N. and **Stemmerik, L.** 1999: Basin evolution in southern East Greenland: an outcrop analog for Cretaceous-Paleogene basins on the North Atlantic volcanic margins. *AAPG Bulletin* 83, 1236–61.

Malmberg, S.-A. 1969: Hydrographic changes in the waters between Iceland and Jan Mayen in the last decade. *Jøkull* 19, 30–43.

McPhee, M.G., Stanton, T.P., Morison, J.H. and **Martinson, D.G.** 1998: Freshening of the upper ocean in the Arctic: is perennial sea ice disappearing? *Geophysical Research Letters* 25, 1729–32.

Mysak, L.A. and **Power, S.B.** 1991: Greenland sea ice and salinity anomalies and interdecadal climate variability. *Climat. Bull.* 25, 81–91.

Nesje, A. and **Dahl, O.** 1993: Lateglacial and Holocene glacier fluctuations and climate variations in western Norway: a review. *Quaternary Science Reviews* 12, 255–61.

O'Brien, S.R., Mayewski, P.A., Meeker, L.D., Meese, D.A., Twickler, M.S. and **Whitlow, S.I.** 1995: Complexity of Holocene climate as reconstructed from a Greenland ice core. *Science* 270, 1962–64.

Ogilvie, A.E.J. 1984: The past climate and sea-ice record from Iceland. Part 1: data to A.D. 1780. *Climatic Change* 6, 131–52.

Ogilvie, A.E.J., Barlow, L.K. and **Jennings, A.E.** 2000: North Atlantic climate *c.* AD 1000. *Weather* 61, 233–51.

Osterman, L.E. and **Nelson, A.** 1989: Latest Quaternary and Holocene paleoceanography of the eastern Baffin Island continental shelf, Canada: benthic foraminiferal evidence. *Canadian Journal of Earth Sciences* 26, 2236–48.

Ostermann, D.R., Curry, W.B., Olafsson, J. and **Honjo, S.** 1998: Variability of foraminiferal flux and isotopic composition at sites around Iceland and the Sea of Okhotsk, with special focus on *N. pachyderma* (sinistral and dextral), *G. quinqueloba* and *G. bulloides.* Abstract from *International Workshop on Environmental and Climate Variations and their Impact in the North Atlantic Region,* 23–26 September 1998.

Paillard, D., Labeyrie, L. and **Yiou, P.** 1996: Macintosh program performs time-series analysis. *EOS* 77(39), 379.

Pflaumann, U., Duprat, J., Pujol, C. and **Labeyrie, L.D.** 1996: SIMMAX: A modern analog technique to deduce Atlantic sea surface temperatures from planktic foraminifera in deep-sea sediments. *Paleoceanography* 11, 15–35.

Rodwell, M.J., Rowell, D.P. and **Folland, C.K.** 1999: Oceanic forcing of the wintertime North Atlantic Oscillation and European climate. *Nature* 398, 320–23.

Rothrock, D.A., Kwok, R. and **Groves, D.** 2000: Satellite views of the

Arctic Ocean freshwater balance. In Lewis, E.L., Jones, E.P., Lemke, P., Prowse, T.D. and Wadhams, P., editors, *The freshwater budget of the Arctic Ocean*. Boston; Kluwer, 409–51.

Serreze, M.C., Maslanik, J.A., Barry, R.G. and **Demaria, T.L.** 1992: Winter atmospheric circulation in the Arctic Basin and possible relationships to the Great Salinity Anomaly in the Northern North Atlantic. *Geophysical Research Letters* 19(3), 293–96.

Sigtryggsson, H. 1972: An outline of the sea-ice conditions in the vicinity of Iceland. *Jøkull* 22, 1–11.

Smith, L.M. 1997: Late Quaternary glaciomarine sedimentation in the Kangerlussuaq region, East Greenland, 68°N. MS thesis, University of Colorado, Boulder, 190 pp.

Smith, L.M. and **Licht, K.** 2000: Radiocarbon date list IX. INSTAAR Occasional Paper, University of Colorado, Boulder.

Stuiver, M., Reimer, P.J., Bard, E., Beck, J.W., Hughen, K.A., Kromer, B., McCormack, F.G., van der Plicht, J. and **Spurk, M.** 1998: INTCAL98 radiocarbon age calibration 24,000–0 cal. BP. *Radiocarbon* 40, 1041–83.

Syvitski, J.P.M., Andrews, J.T. and **Dowdeswell, J.A.** 1996: Sediment deposition in an iceberg-dominated glacimarine environment, East Greenland: basin fill implications. *Global and Planetary Change* 12, 251–70.

Tremblay, L.B., Mysak, L.A. and **Dyke, A.S.** 1997: Evidence from driftwood records for century-to-millennial scale variations of the high latitude atmospheric circulation during the Holocene. *Geophysical Research Letters* 24(16), 2027–30.

Williams, K.M., Andrews, J.T., Jennings, A.E., Short, S.K., Mode, W.N. and **Syvitski, J.P.M.** 1995a: The Eastern Canadian Arctic at ca. 6 ka: a time of transition. *Geographie Physique et Quaternaire (Canadian Global Change issue)* 49(1), 13–27.

Williams, K.M., Andrews, J.T. and **Weiner, N.J.** 1995b: Late Quaternary Paleoceanography of the mid- to outer Continental Shelf, East Greenland. *Arctic and Alpine Research* 27(4), 352–63.